Title: Gaseous and particulate pollutant emissions from ocean-going tankers in the context of carbon reduction： main engine, auxiliary engine, and auxiliary boiler

Song Zhou[a], Ang Sun[a], Chunjing Lou[b], Peilin Zhou[c,d], Hongyuan Xi[a]*, Majed Shreka[a], Haibin Wang[c], Yuanqing Zhu[a], Yongming Feng[a]

[a] College of Power and Energy Engineering, Harbin Engineering University, Harbin 150001, China

[b] Shanghai Waigaoqiao Shipbuilding Co., Ltd., Shanghai 200137, China

[c] Department of Naval Architecture, Ocean and Marine Engineering, University of Strathclyde, Glasgow, G4 0LZ, UK

[d] Faculty of Marine Science and Technology, Harbin Institute of Technology, Weihai, 264209, China

corresponding author: Hongyuan Xi

E-mail address: xhy_9999@163.com

Abstract: Ships are a major source of air pollution, which significantly impacts global health. In this study, the gaseous and particulate emissions from the main engine, auxiliary engine, and auxiliary boiler of a modern Tier III large ocean-going vessel fueled with marine gas oil and heavy fuel oil have been investigated. Emissions of gaseous pollutants in the exhaust were measured online and particulate samples were collected to determine detailed physical and chemical properties. The results indicated that CO_2 and NOx are the main gaseous pollutants, while organic carbon accounts for the majority of particulate pollutants for the three devices. The element carbon emissions of the auxiliary engine decreased with load increasing while those of the main engine maintained a level of approximately 0.062 g/kWh. The black carbon emissions of the main and auxiliary engine resulting from using marine gas oil were higher than heavy fuel oil. Consistent correlations among pollutants were observed for the engines. Finally, the measured value of element carbon cannot be utilized as a substitute for black carbon emissions due to the presence of light-absorbing organic carbon in organic carbon.

Keywords: Marine diesel engine; Gaseous pollutants; Particle emissions; Heavy fuel oil; Marine gas oil; Pearson correlation.

Abbreviations			
AAE	Angstrom Absorption Exponent	MGO	marine gas oil
BC	black carbon	NDIR	non-dispersive infrared
DOC	diesel oxidation catalysts	NOx	nitrogen oxides
CLD	chemiluminescence detection method	OC	organic carbon
CO_2	carbon dioxide	PAHs	polycyclic aromatic hydrocarbon
EC	elemental carbon	PM	particulate matter
ECAs	emission control areas	SCR	selective catalytic reduction
HFO	heavy fuel oil	SFOC	Specific Fuel OilConsumption
HVO	Hydrotreated Vegetable Oils	SLCF	short-lived climate forcing
IMO	International Maritime Organization	SOx	sulfur oxides

1 Introduction

As the economy recovers, the role of the shipping industry in the global transport of goods has become increasingly critical. Ship transportation accounts for over 80% of international trade transportation [1]. However, ships' pollutants have also become an essential source of marine pollution, especially in offshore areas. About 8% of sulfur oxides (SOx), 15% of nitrogen oxides (NOx), and about 3% of the world's carbon dioxide (CO_2) come from ship emissions [2]. In addition to the above-mentioned gas-phase pollutants, the emission of particulate matter from ships also dramatically impacts the marine environment [3].

To reduce the emissions of ships, the International Maritime Organization (IMO) has set up emission control areas (ECAs) in specific coastal regions. Only ships using fuels with a sulfur content of less than 0.1% wt are allowed in the ECAs, while 0.5% wt sulfur content can be used outside the ECAs [4]. As the shipping industry gradually transitions towards carbon reduction and decarbonization, novel low-carbon and zero-carbon fuels are being implemented on ships. Due to its lack of carbon atoms in its chemical structure, hydrogen exhibits high flammability, diffusivity, and minimal carbon emissions. By precisely adjusting the nozzle diameter and spray cone angle, the combustion performance and emission characteristics of hydrogen-diesel dual-fuel engines can be effectively enhanced[5]. Furthermore, the utilization of hydrogen/biodiesel blended fuel can further optimize both combustion performance and emission attributes of dual-fuel engines[6]. Additionally, Hydrotreated Vegetable Oils (HVO) offer a viable option for achieving short-term and medium-term emission reductions as they can be used without necessitating changes to the engine fuel system[7, 8]. Moreover, employing exhaust after-treatment technologies such as diesel oxidation catalysts (DOC) along with selective catalytic reduction (SCR) techniques provides an opportunity for additional pollutant emission reduction while meeting increasingly stringent regulations[9]. Despite the gradual adoption of novel clean energy technologies in ocean-going vessels, heavy fuel oil (HFO) remains the predominant fuel for ship diesel engines due to cost considerations[10]. To meet the stringent emission regulations, ships using HFO are often required to use exhaust aftertreatment technology to meet the needs of relevant regulations[11]. IMO has only developed applicable regulations for SOx and NOx, while there are still no uniform regulations on diesel particulate matter [12]. With the gradual improvement of the relevant rules on SO_2 and NO_x, the particulate matter emissions from marine diesel engines have gradually attracted the attention of all countries worldwide.

There are numerous factors that can impact ship emissions, such as the type of fuel used, and the engine loading employed. Studies have shown that ship emissions are greatly affected by changes in the load of marine diesel engines. The changes in load affect fuel combustion in the cylinder, which in turn impacts the generation of emissions [13]. In addition, different operating conditions of ships affect the load of engines. The diesel engine usually operates at a lower load when the ship enters and leaves ports, while medium loads are typically used on high seas. When entering and leaving the dock, ships' gaseous pollutants and particulate matter are significantly higher than on high seas [14].

The fuel type is also an essential factor affecting diesel engine pollutant emissions [15]. HFO has a high density and viscosity and contains high impurities, ash, and sulfur [16]. Therefore, when using HFO, the emissions of gaseous pollutants and particulate matter in the ship will be higher than when using Marine Gas Oil (MGO) [17]. Meanwhile, the emissions of particulate matter (PM) and polycyclic aromatic hydrocarbons (PAHs) from HFO are higher than MGO, which increases the impact of ship pollutants on human health [18].

The boilers which produce steam and hot water are also an essential source of ship emissions. However, there are few regulations for boilers. When entering the ECAs and ports, the ships reduce the emissions of the boilers by switching to MGO only.[19] The emissions of the boilers are low, which accounts for less than 5% of ship emissions [20].

In summary, a substantial body of literature exists on ship emission characteristics. However, these studies primarily focus on the emissions of engines utilizing a single fuel, with limited research conducted on the emission disparities between different fuels. Furthermore, previous investigations predominantly rely on bench experiments, and there are a few emission measurements from ships during actual voyages. Additionally, there remains an inadequate understanding of the emission characteristics exhibited by various burners installed on the same vessel. To gain deeper insights into mechanisms governing pollutant formation, it is crucial to obtain more comprehensive emission data that elucidates the influence of both fuel types and combustion devices.

In this paper, the emissions of pollutants from an ocean-going vessel utilizing HFO and MGO have been investigated. Besides, the measurement of gaseous pollutants such as CO_2, NOx, and SOx emitted by both the main engine and auxiliary engines during navigation was encompassed in this study. Additionally, significant attention was given to examining particulate pollutants including elemental carbon (EC), organic carbon (OC), and black carbon (BC). It is noteworthy that the potential of OC/EC as a tracer for fuel sources and its impact on BC measurements was also explored. For boilers, the primary focus was placed on analyzing their emissions of various pollutants when using HFO. Furthermore, the correlations between different types of pollutants were investigated.

2. Experimental process and methods

2.1 Engine and fuel properties

The study was conducted on an Aframax crude oil tanker, which has a deadweight capacity of 114000 tons. The total length and width of the vessel are 250 meters and 44 meters, respectively. In addition, it is outfitted with a single main engine, along with three auxiliary engines and one boiler.

The main engine is a Tier III 6-cylinder MAN-6G60ME-C9.5-HPSCR two-stroke engine, while the auxiliary engine is the DAIHATSU 6DE-20 medium-speed diesel four-stroke engine. The engine parameters are listed in **Table 1**. Meanwhile, the information of the experimental devices is shown in Table 2. The fuel consumption of the boiler is 131.5 kg/h. HFO 180 and MGO were used for the test, their specific parameters are presented in Table 3.

Table 1 Technical Parameters of the test engines

	Main Engine	Auxiliary Engine
Engine type	Two-stroke engine	Four-stroke engine
No. of cyl	6	6
power (kW)	13500	900
speed (rpm)	91.1	900
bore (mm) × stroke (mm)	600 × 2790	205 × 300
Specific Fuel Oil Consumption (SFOC)	152 g/kWh+5%	
Dry weight（ton）	534	16

Table 2 the information of the experimental devices

Measured variable	Position	Sensor-device principle	Type	Accuracy
Fuel mass flow	Fuel line	Gravimetric meter	AVL / 733	± 0.12%
Temperature	Exhaust line	Thermocouple	TC direct	± 2.5 °C
NO_x, CO, SO_2, O_2, CO_2	Exhaust line	CLA, NDIR, PMA	Horiba PG 350	±0.5% of the full-scale
BC	Exhaust line	Optical	AVL / 415SE	± 0.025 FSN
pressure	Exhaust line	Piezoresistive transducer	Kistler 4049	± 0.3% FS

Table 3 Tested fuel properties

	MGO	HFO 180
Water (%mass)	0	0.09
Kinematic viscosity (mm^2/s, 20°C)	4.72	152.3
Mechanical impurities (%)	0	0.132
Density (g/ml)	0.8343	0.979
Flashpoint (°C)	72.5 (101.3 kPa)	112 (101.3k Pa)
Gross calorific value (MJ/kg)	45.72	42.62
Net calorific value (MJ/kg)	42.71	40.28
Sulfur(mass%)	0.0229	0.432

This is the author accepted manuscript of the article: Zhou, S., Sun, A., Lou, C., Zhou, P., Xi, H., Shreka, M., Wang, H., Zhu, Y., & Feng, Y. (2024). Gaseous and particulate pollutant emissions from ocean-going tankers in the context of carbon reduction: main engine, auxiliary engine, and auxiliary boiler. *Energy*, *313*, Article 133831. https://doi.org/10.1016/j.energy.2024.133831. For the purposes of open access, a CC BY 4.0 licence has been applied to this manuscript.

2.2 Emissions Sampling and Analytical Methods

Due to practical limitations in conducting comprehensive condition testing during actual navigation, experiments were conducted on the main engine within a load range of 25% to 90%, adhering to ISO 8178-4 E3 test cycle. The auxiliary engine was operated within a load range of 25% to 85%, following ISO 8178-4 D2 cycle.

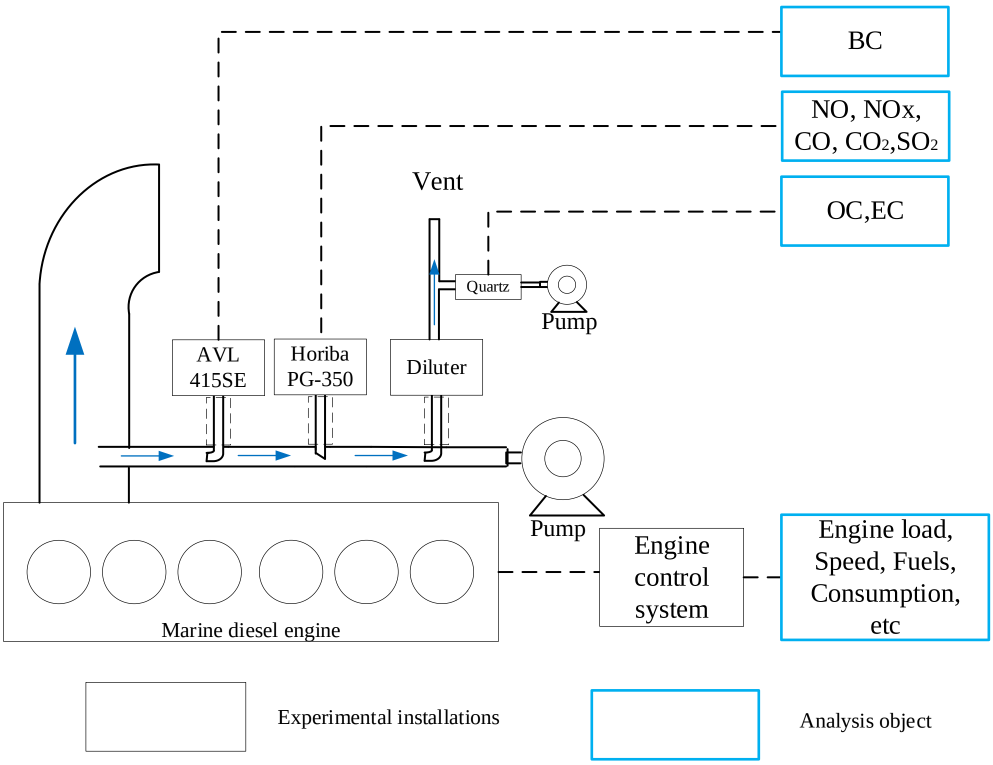

Figure 1 Schematic diagram of the sampling system

Figure 1 illustrates the sampling system. To ensure the stability of exhaust gas, sampling orifices were positioned at a distance approximately 6-10 times the diameter of the turbocharger. The gaseous pollutant emissions from diesel engines were quantified using an exhaust gas analyzer (Horiba, PG-350, Japan) employing the non-dispersive infrared (NDIR) spectroscopic method and chemiluminescence detection method (CLD), respectively. The measured pollutants included SO_2, CO_2, CO, and NOx. Prior to measurement, the analyzer was calibrated for zero point and total range using standard gases. BC measurements were conducted using AVL 415SE, while PM carbon composition was collected utilizing a quartz membrane sampler. The exhaust gas is diluted in the sampling tube through the diluter. The dilution rate is determined according to the change in NOx concentration before and after dilution to ensure that the dilution rate is between 6-8.. The PM was then collected from the diluted exhaust gas utilizing a 47 nm quartz filter membrane sampler with a duration of 30 minutes.

EC and OC were obtained from samples collected using quartz filter membranes. Prior to sampling, the filter membranes were subjected to a 5-hour heating process at 500 ℃ in a muffle furnace to eliminate moisture and carbon-containing pollutants. The quantification of EC and OC was achieved by subjecting the samples to varying temperatures using a thermal/optical carbon aerosol analyzer.

Results and discussion

3.1. Gaseous emissions

The NOx emissions from various combustion devices in the tested vessel are depicted in Figure 2. Meanwhile the emission factor (g/kWh) of gaseous emissions are shown in Table 4. When utilizing HFO, the main engine's NOx emissions ranged from 69.74±3.7 g/kg fuel to 110.5±4.8 g/kg fuel, while those of the auxiliary engine ranged from 42.4±1.7 g/kg fuel to 47.9±1.9 g/kg fuel. The NOx generated by diesel engines primarily originates from thermal NOx formation, which predominantly occurs in high-temperature regions and is influenced by temperature, excess air coefficient, and residence time within the high-temperature zone [21]. Due to longer combustion duration and higher excess air coefficient, two-stroke diesel engines exhibit higher levels of NOx emissions compared to four-stroke auxiliary engines. In addition, fuel type is also an important factor affecting NOx emissions. When burning HFO, NOx emissions are higher compared to MGO. In contrast to HFO, MGO exhibits a shorter ignition delay due to its lower density and viscosity, resulting in a reduced peak flame temperature and mitigated NOx formation [22]. Moreover, the decreased nitrogen content in MGO contributes to the reduction of NOx emissions [23]. However, a significant decrease in NOx emissions below 5 g/kWh has been achieved through the utilization of SCR's catalytic oxidation process.

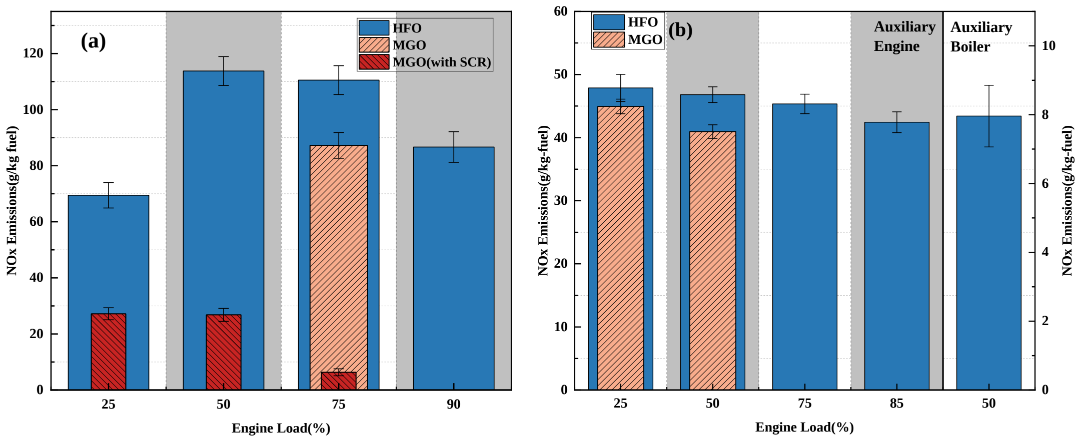

Figure 2. (a–b): NOx emissions：(a) main engine, (b) auxiliary engine and boiler

This is the author accepted manuscript of the article: Zhou, S., Sun, A., Lou, C., Zhou, P., Xi, H., Shreka, M., Wang, H., Zhu, Y., & Feng, Y. (2024). Gaseous and particulate pollutant emissions from ocean-going tankers in the context of carbon reduction: main engine, auxiliary engine, and auxiliary boiler. *Energy*, *313*, Article 133831. https://doi.org/10.1016/j.energy.2024.133831. For the purposes of open access, a CC BY 4.0 licence has been applied to this manuscript.

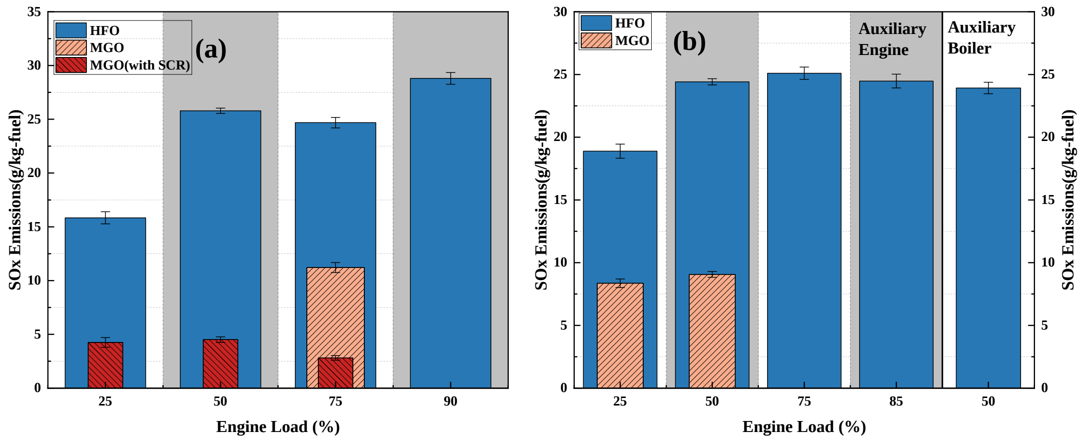

Figure 3. (a–b): SO_2 emissions: (a) main engine, (b) auxiliary engine and auxiliary engine.

The ship's SO_2 emissions primarily originate from fuel, with a minor contribution from lubricating oil [24]. In addition, the sulfur content of HFO surpasses that of MGO, which explains why the SO_2 emissions from MGO are lower than those from HFO [25].

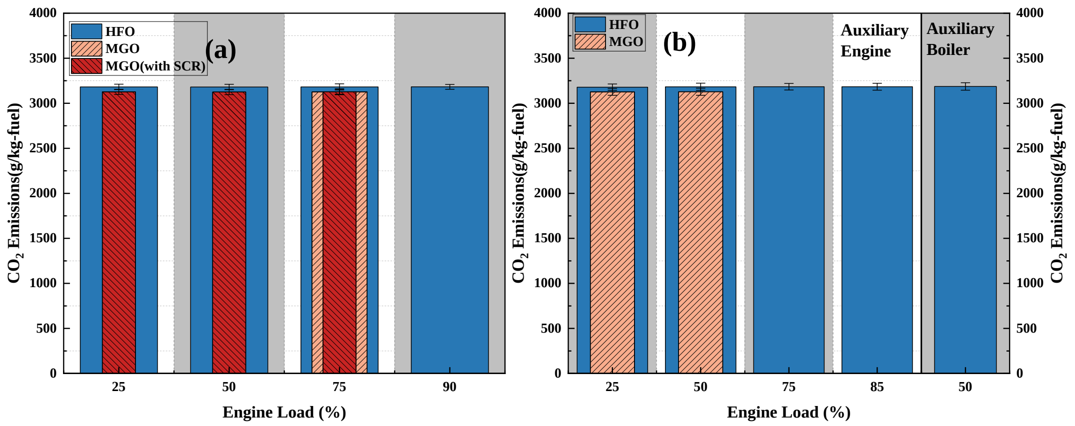

Figure 4. (a–b): CO_2 emissions: (a) main engine, (b) auxiliary engine and auxiliary boiler

Figure 4 illustrates the CO_2 emissions, which remain largely invariant to variations in load and engine type. Notably, the CO_2 emissions are marginally elevated when HFO is utilized in comparison to MGO. The CO_2 emissions of the boiler are approximately 3180 g/kg of fuel, which aligns with findings from previous studies [26].

Table 4 the Gaseous emissions (g/kWh) of main engine and auxiliary engine

	Fuel	Load	NOx	NO_2	NO	SOx	CO_2	CO
Main Engine Emission Factors (g/kWh)	HFO	25%	12.35±0.77	6.36±0.44	5.99±0.14	2.55±0.09	550±6.07	0.41±0.25
		50%	20.15±0.91	5.43±0.56	14.72±0.35	4.65±0.04	597±5.71	0.36±0.12
		75%	20.01±0.90	3.97±0.29	16.04±0.56	4.17±0.09	560±6.20	0.40±0.11
		90%	14.8±0.96	2.54±0.10	12.26±0.80	4.89±0.10	548±4.68	0.41±0.11
	MGO	75%	13.81±0.75	3.28±0.25	10.52±0.42	1.93±0.78	507±4.18	0.84±0.21
	MGO (with SCR)	25%	4.27±0.35	3.43±0.16	0.85±0.15	2.89±0.07	508±4.89	0.31±0.15
		50%	4.74±0.41	0.79±0.15	3.94±0.21	0.88±0.04	558±5.12	1.28±0.21
		75%	1.44±0.21	0.30±0.11	1.13±0.05	0.27±0.34	521±5.35	0.79±0.32
Auxiliary Engine Emission Factors (g/kWh)	HFO	25%	11.07±0.63	2.23±0.12	8.84±0.47	4.41±0.15	735.28±3.11	1.51±0.08
		50%	10.84±0.43	1.35±0.15	9.50±0.12	5.51±0.21	733.18±2.67	0.57±0.11
		75%	10.17±0.27	1.31±0.07	8.86±0.23	5.64±0.11	719.43±2.82	0.58±0.08
		85%	9.77±0.34	1.43±0.09	8.34±0.17	5.64±0.18	716.19±2.44	0.55±0.03
	MGO	25%	10.71±0.33	0.9±0.18	9.81±0.14	2.01±0.14	743.66±5.11	0.77±0.02
		50%	10.12±0.56	1.11±0.17	9.02±0.33	2.15±0.13	770.62±4.81	0.85±0.02

3.2. Emission factors of carbonaceous matter at different operating loads

The PM emitted by diesel engines primarily consists of OC, EC, and various metal salt impurities [27]. Among these components, the dominant constituents of PM are carbonaceous particles mainly composed of OC and EC.

The emissions of EC and organic carbon OC from both the main and auxiliary engines are depicted in Figure 5. Regarding the main engine, OC accounts for the majority of carbonaceous particle emissions at approximately 92-96%, while EC only contributes to around 4%-8%. It is worth noting that multiple factors influence the formation of OC in engine emissions. However, research has indicated that incomplete combustion of hydrocarbon molecules in fuel and leakage of lubricating oil during sweeping are among the primary contributors to the generation of carbonaceous particle emissions [28, 29]. With an increase in load, carbonaceous particle emissions from HFO initially rise, reaching their peak at a load of 75%, followed by a decline. Compared to HFO, MGO exhibits lower levels of carbonaceous particle emissions. Due to the high concentration of hydrocarbon fuels in HFO, complete combustion becomes difficult during the combustion process [30]. Consequently, unburned hydrocarbons gradually transform into OC within the exhaust gas. Additionally, once an SCR system is employed, there is a significant reduction in both OC and EC concentrations. This phenomenon can be attributed to the porous structure inherent in SCR carriers which effectively intercept carbonaceous particles.

For the auxiliary engine, the proportion of EC in carbonaceous particles is higher compared to that of the main engine, and the EC ratio exhibits different trends depending on the fuel type. From Figure 5 (b), when using HFO, the proportion of EC is most prominent at low loads and gradually decreases as the load increases. In addition, there is a higher proportion of EC at 25% engine load compared to that at 50% load when using MGO. Moreover, the majority of carbonaceous particles in the auxiliary boiler are composed of OC.

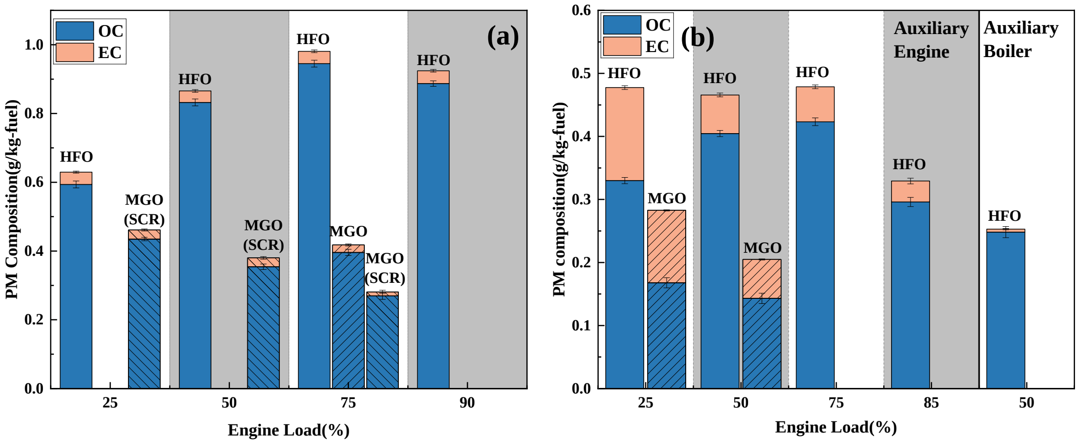

Figure 5. Carbonaceous particle emissions: (a) main engine, (b) auxiliary engine and auxiliary boiler

The emissions of OC and EC with engine loads are shown in Figure 6 (a). The emission of OC demonstrates a similar trend to the engine loads when different engines operate on the same fuel. Notably, the use of MGO effectively reduces OC emissions compared to HFO. When using HFO, OC emission exhibits an upward trend as the load increases from 25% to 75% and then a downward trend as the engine load continues to increase to 90%. Conversely, when MGO is used in the auxiliary engine, The OC emissions decrease with the increasing load. Moreover, SCR has proven to be highly effective in reducing OC emissions by 35%.

The EC emissions of the auxiliary engine are higher than those of the main engine, as shown in Figure 6 (b). This phenomenon can be attributed to the elevated fuel-air ratio of the two-stroke diesel engine, which reduces the formation of high-temperature and hypoxic regions within the cylinder. The EC emissions for the main engine remain at a level of approximately 0.035 ± 0.003 g/kg fuel when using HFO. As for the auxiliary engine, there is a decline in EC emissions as load increases for both fuel types. These findings align with previous research that demonstrated how higher engine loads lead to lower EC emissions due to improved combustion efficiencies [31].

The differences in EC emissions between the two types of engines can be attributed to the inherent structural distinctions between two-stroke and four-stroke engines. As for the four-stroke engines, an increase in load results in higher in-cylinder temperature and excess air coefficient, consequently leading to a reduction in EC formation. Conversely, variations in excess air coefficient have minimal impact on EC generation for two-stroke engines. Furthermore, due to its moderate structure, SCR technology demonstrates a significant potential for reducing EC emissions.

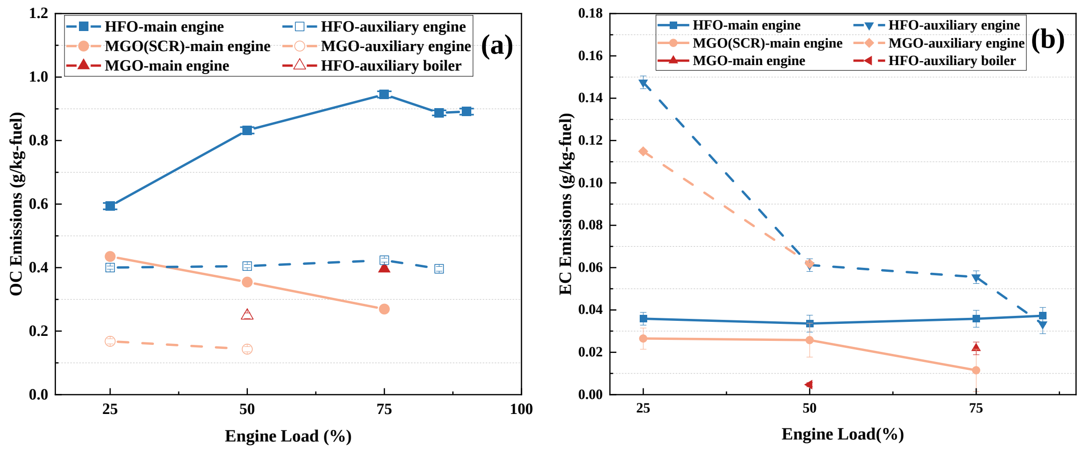

Figure 6. EC and OC emissions: (a) main engine, (b) auxiliary engine and auxiliary boiler

The OC/EC ratio is commonly employed in the analysis of atmospheric particulate matter sources to ascertain their origin and association with PM [32]. Notably, the OC/EC ratio exhibits a wide range of variation for marine diesel engines, as illustrated in Figure 7. For HFO, the average OC/EC is found to be 23.34 while that of the MGO is 17.9. In contrast, the OC/EC of the auxiliary engine for both fuel types is considerably lower ranging from 1.4 to 9. In this case, the average OC/EC value when using HFO and MGO is determined as 6.34±2.89 and 2.07±0.86, respectively. The results further indicate that there exists a significant disparity between two-stroke and four-stroke engines regarding their respective levels of OC/EC emissions. Compared to the case when

MGO is used as fuel for the main engine without the SCR system, the OC/EC ratio after using the SCR system increases due to a substantial reduction in EC concentration.

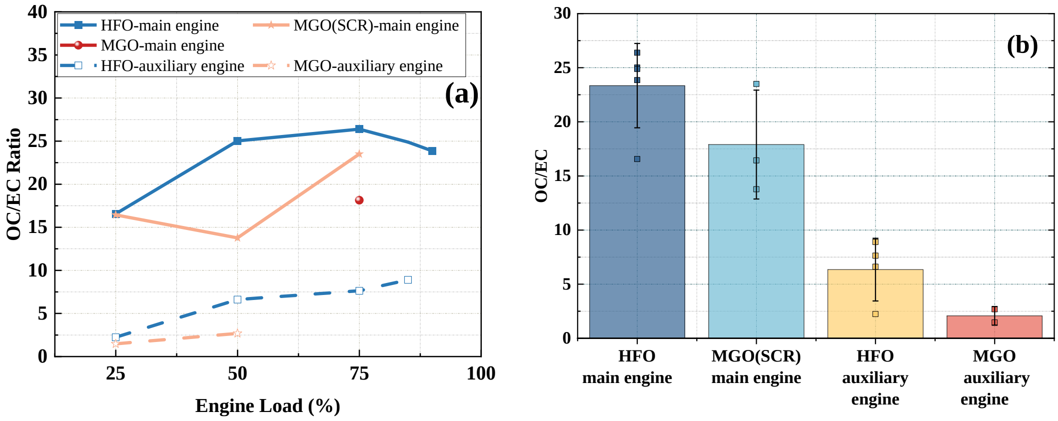

Figure 7. EC/OC ratio at different loads: (a) the main engine, (b) the auxiliary engine

There are significant variations in the OC/EC ratio among different sources. Typically, biomass combustion yields a higher OC/EC ratio compared to fossil fuel combustion [33, 34]. Figure 8 illustrates the OC/EC ratio of carbonaceous particles from diverse sources [35, 36]. In this study, the main engine exhibits the highest OC/EC ratio ranging from 13.8 to 25. The OC/EC ratio of biomass burning is higher than that of road vehicles, while the auxiliary engine shows similar levels as road vehicles. The use of gasoline results in a higher OC/EC ratio compared to diesel. When biodiesel is used as fuel for two-stroke diesel engines, the OC/EC ratio significantly decreases compared to conventional fuels and becomes similar to that observed in four-stroke diesel engines using MGO.

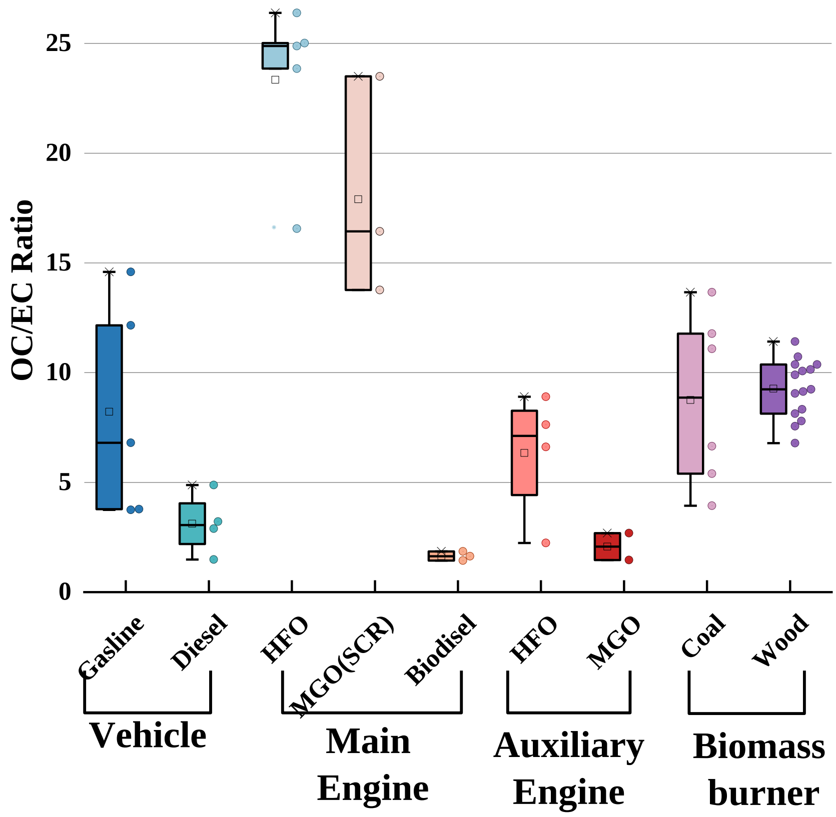

Figure 8. OC/EC ratio of carbonaceous particles from different sources

BC exhibits strong absorption of visible light and is resistant to chemical migration. In contrast to carbon dioxide and methane, BC is recognized as a significant short-lived climate forcing (SLCF) substance, with its climate impact diminishing rapidly upon the cessation of emissions [37]. BC released into the atmosphere absorbs light and radiates it back into the surrounding atmosphere, thereby affecting the global climate. In particular, BC emissions north of the 40th parallel are attributed to marine shipping activities, which are assumed to be a significant source contributor to BC emissions in the Arctic [38]. The BC emissions of the main engine, the auxiliary engine, and the auxiliary boiler are shown in Figure 9.

As the load increases, there is an initial decline followed by a subsequent rise in BC emissions.

This is the author accepted manuscript of the article: Zhou, S., Sun, A., Lou, C., Zhou, P., Xi, H., Shreka, M., Wang, H., Zhu, Y., & Feng, Y. (2024). Gaseous and particulate pollutant emissions from ocean-going tankers in the context of carbon reduction: main engine, auxiliary engine, and auxiliary boiler. *Energy*, *313*, Article 133831. https://doi.org/10.1016/j.energy.2024.133831. For the purposes of open access, a CC BY 4.0 licence has been applied to this manuscript.

At lower engine loads, the reduced cylinder temperature leads to a decrease in fuel thermal efficiency and consequently results in the generation of unburned fuel and lubricating oil, which significantly contributes to BC emissions. Additionally, the BC emissions from MGO surpass those from HFO at 75% engine load. This phenomenon can be attributed to the presence of metallic impurities and metals in HFO, which facilitate the combustion-induced oxidation of BC within the cylinder [39]. However, the BC emissions for the auxiliary engine decrease with the load increase, which is different from the main engine. This result is in line with the results of C. McCaffery et al [40]. Furthermore, similar to the main engine, the auxiliary engine's BC emissions are higher when using MGO compared to HFO.

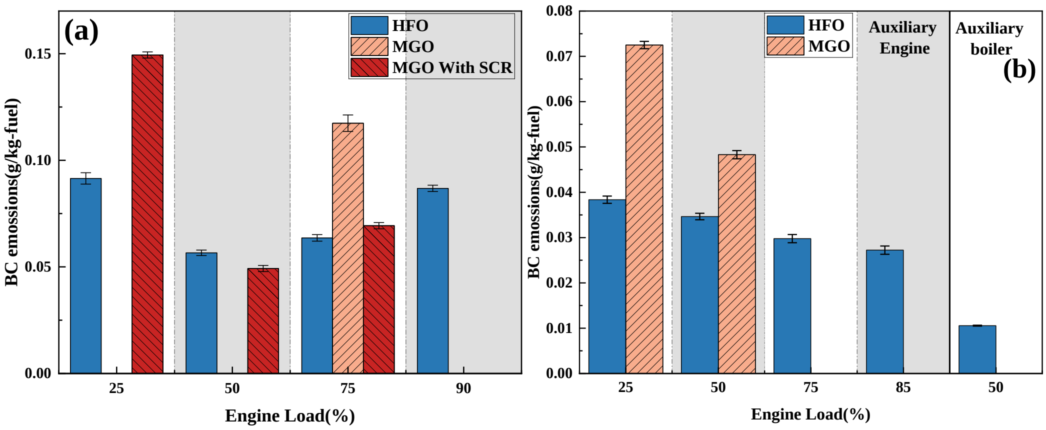

Figure 9. BC emissions: (a) the main engine; (b) the auxiliary engine and the auxiliary boiler

3.3. Effect of OC on EC and BC measurements

It has been reported that EC emissions are commonly employed as a substitute for BC emissions to assess the ship's environmental impact [41]. However, there are some differences between the BC and the EC [42]. Additionally, OC will also have an impact on the measurement of BC, due to the BrC, which is a type of organic carbon that absorbs light. In this study, the relationship between BC and EC exhibits a dynamic correction trend under different operating conditions. For the main engine, the Pearson correlation coefficient of HFO is 0.3 (n=6), while that of MGO is 0.6 (n=5). In the case of the auxiliary engine, the Pearson correlation coefficient of the HFO is 0.1 (n=5), lower than that of the main engine. However, due to insufficient data on auxiliary engines using MGO, reliable correlation coefficients could not be obtained.

Due to the effect of BrC, there is a significant difference in BC emissions under the same EC emissions, as shown in Figure 10. When the OC/EC ratio is bigger than 16, the BC/EC ratio is more than 1. In contrast, the BC/EC ratio is less than 1 when the OC/EC ratio is smaller than 10. This is because the AVL 415SE is a filter-based instrument, and is thus subject to the filter artifact which would enhance the light absorption of BC and increase the reported BC value compared to the instrument-average [43]. On the other hand, there is a large amount of tar BrC in OC, which is an amorphous spherical carbon. It is composed of macromolecular substances predominantly characterized by highly conjugated aromatic rings, such as polycyclic. The light absorption of BrC in the short-wave range is significantly enhanced compared to small molecule organics, owing to polyaromatic ring structure and a high degree of polymerization. In comparison to BC, BrC exhibits higher Angstrom Absorption Exponent (AAE) values and a greater ratio of sp3 to sp2 carbon bonds [44].

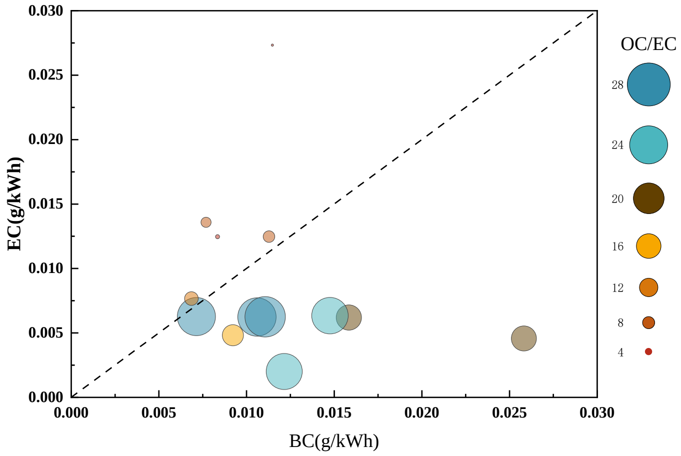

Figure 10. Relationship between emission factors of EC and BC with OC/EC ratios categorized by value.

3.4 Relationship between measured exhaust gases and particulate emissions

The gaseous and particulate pollutant emissions based on fuel consumption at 50% load for different diesel engines are shown in Figure 11. The emissions of CO_2, CO, and SO_2 remain unaffected by the engine type, potentially due to their predominantly originating from the fuel in the exhaust gas. In terms of NOx emissions, the main engine exhibits the highest levels, followed by the auxiliary engine, and then the auxiliary boiler. Thermal NOx constitutes the primary component of NOx emissions from diesel engines, contributing up to 80%. The high NOx emissions of the main engine may be attributed to the elevated air coefficient and prolonged combustion duration of two-stroke engines. The BC and OC show the same trend as the NOx. Moreover, the particulate pollutants emitted by diesel engines exhibit higher levels compared to those emitted by auxiliary boilers. In addition, the main engine emits elevated levels of BC and OC in comparison to the auxiliary engine, while demonstrating lower levels of EC.

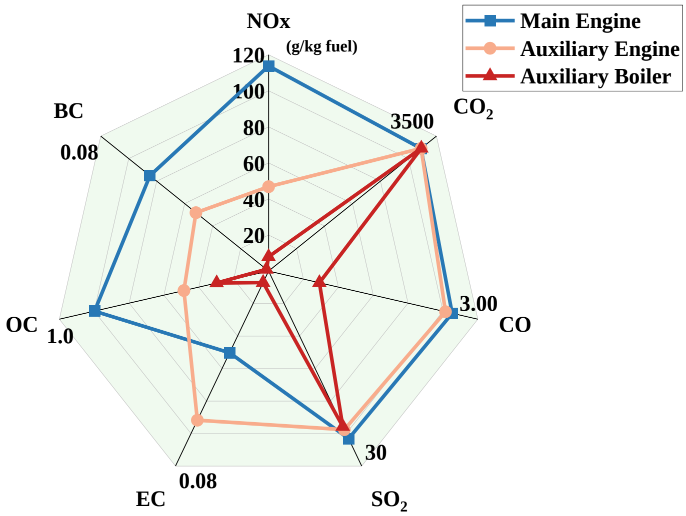

Figure 11. Gaseous and particulate pollutant emissions resulted from using HFO for different diesel engines at 50% load.

It is valuable to monitor the emissions of exhaust gases and conduct a comparative analysis between their levels and the concentrations of particulate pollutants. However, due to space and cost limitations, measuring all pollutants, particularly particulate pollutants, can be challenging. In addition, gas pollutants are primarily detected using online methods that provide real-time emission data, whereas offline methods are mostly used for detecting particulate pollutants. Therefore, the relationship between different pollutants can be studied to predict the emission levels of related pollutants, utilizing easily measurable pollutants as indicators. The major gas pollutants, including CO, CO_2, NO, NO_2, and SO_2, are compared alongside the major particulate pollutants OC and EC. The Pearson coefficient is used to determine the degree of correlation between the pollutant. The P-value represents the probability of the correlation coefficient r being zero. A smaller p-value indicates a larger correlation coefficient r, indicating a stronger correlation [45].

The correlations between the gas pollutants and the particulate pollutants emitted by the main engine and auxiliary engine are shown in Figure 12. Notably, there is a consistent trend in correlations for certain pollutants across both fuels. CO_2 exhibits a strong positive correlation with NOx. And CO shows a strong positive correlation with EC. This is because both CO and EC are products of incomplete combustion. Since NOx is mainly composed of NO, NOx also has a significant positive correlation with NO.

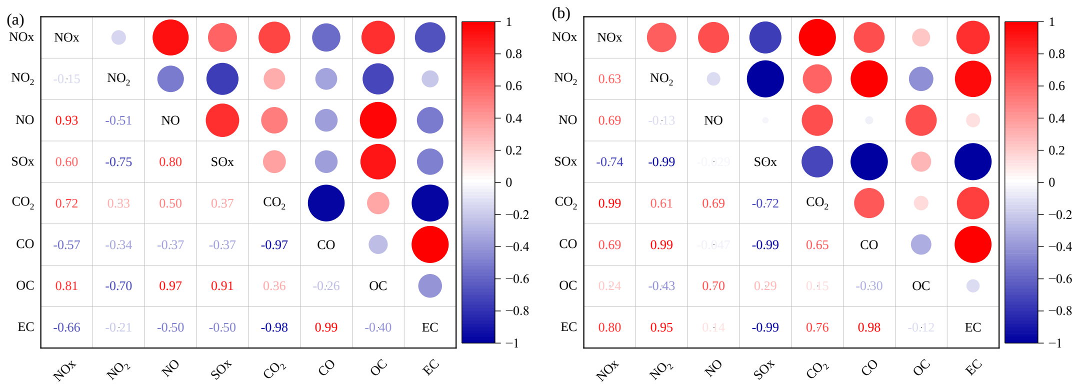

Figure 12 Correlations among gas and particulate pollutants: (a) main engine, (b)auxiliary engine

4 Conclusions

In this study, the gaseous and particulate emissions originating from the main engine, auxiliary engine, and boiler of a Tier III ship powered by MGO and HFO have been investigated. The main conclusions are as follows:

(1) The type of fuels and engines significantly influenced pollutant emissions. Gaseous pollutants mainly consisted of CO_2 and NOx, while OC accounted for the majority of particulate pollutants. For the main engine, the gaseous and particulate pollutants emitted by HFO were higher than those emitted by MGO, except for BC. Compared to MGO, utilizing HFO in the auxiliary

engine increased the emissions of OC and SO_2 but reduced the emissions of BC and EC. The pollutants emitted from the boiler exhibited lower levels compared to those emitted by the engines, except for CO, CO_2, and SO_2.

(2) When using HFO, OC emissions from both engines increased until reaching their peak at 75% load before declining. When using MGO, the SCR system effectively reduced OC and EC emissions. Moreover, the PM emitted by the boiler was mainly composed of OC.

(3) The OC/EC ratio varied significantly among different sources. The OC/EC ratio of the main engine exceeded 13, while that of the auxiliary engine ranged from 1.4 to 9. Both engines exhibited higher OC/EC ratios when using HFO compared with MGO.

(4) The presence of light-absorbing organic carbon in OC led to a significant discrepancy between the measured BC value and EC. An OC/EC ratio exceeding 16 yielded a BC/EC ratio greater than 1, while a ratio below 10 resulted in a BC/EC ratio less than 1.

(5) The correlation of certain pollutants emitted by the main engine and auxiliary engine exhibited consistent trends. CO_2 exhibits a strong positive correlation with NOx. Moreover, CO shows a positive correlation with EC.

The findings of this study can offer valuable data support for the effective regulation of gaseous and particulate pollutant emissions from shipping, the further enhancement of marine fuel policies, and a more precise evaluation of the environmental and climatic impacts resulting from ship emissions within the context of climate change.

Reference

[1] Huang X, Wen Y, Zhang F, Han H, Huang Y, Sui Z. A review on risk assessment methods for maritime

transport. Ocean Engineering. 2023;279:114577.

[2] Chountalas TD, Founti M, Tsalavoutas I. Evaluation of biofuel effect on performance & emissions of a 2-stroke marine diesel engine using on-board measurements. Energy. 2023;278:127845.

[3] Yeh C-K, Tzu F-M, Chen P-Y, Shen H-C, Yuan C-S, Lin C, et al. Emission characteristics of naphthalene from ship exhausts under global sulfur cap. Science of The Total Environment. 2023;902:166172.

[4] Elbaz AM, khateeb AA, Roberts WL. PM from the combustion of heavy fuel oils. Energy. 2018;152:455-65.

[5] Zhang Z, Wang S, Pan M, Lv J, Lu K, Ye Y, et al. Utilization of hydrogen-diesel blends for the improvements of a dual-fuel engine based on the improved Taguchi methodology. Energy. 2024;292:130474.

[6] Tan D, Wu Y, Lv J, Li J, Ou X, Meng Y, et al. Performance optimization of a diesel engine fueled with hydrogen/biodiesel with water addition based on the response surface methodology. Energy. 2023;263:125869.

[7] Di Blasio G, Ianniello R, Beatrice C. Hydrotreated vegetable oil as enabler for high-efficient and ultra-low emission vehicles in the view of 2030 targets. Fuel. 2022;310:122206.

[8] Pellegrini L, Beatrice C, Di Blasio G. Investigation of the effect of compression ratio on the combustion behavior and emission performance of HVO blended diesel fuels in a single-cylinder light-duty diesel engine. SAE Technical Paper; 2015.

[9] Zhang Z, Ye J, Tan D, Feng Z, Luo J, Tan Y, et al. The effects of Fe2O3 based DOC and SCR catalyst on the combustion and emission characteristics of a diesel engine fueled with biodiesel. Fuel. 2021;290:120039.

[10] Qu J, Feng Y, Zhu Y, Wu B, Wu Y, Xiao Z, et al. Assessment of a methanol-fueled integrated hybrid power system of solid oxide fuel cell and low-speed two-stroke engine for maritime application. Applied Thermal Engineering. 2023;230:120735.

[11] Deng J, Wang X, Wei Z, Wang L, Wang C, Chen Z. A review of NOx and SOx emission reduction technologies for marine diesel engines and the potential evaluation of liquefied natural gas fuelled vessels. Science of The Total Environment. 2021;766:144319.

[12] Zhang F, Chen Y, Su P, Cui M, Han Y, Matthias V, et al. Variations and characteristics of carbonaceous substances emitted from a heavy fuel oil ship engine under different operating loads. Environmental Pollution. 2021;284:117388.

[13] Wu M, Zhao Z, Zhang P, Wang X, Liu X, Ni K, et al. Effects of different national standards and driving conditions on pollutants and persistent free radicals in diesel engine exhaust particles. Science of The Total Environment. 2024;907:167880.

[14] Yang L, Zhang Q, Lv Z, Zhao J, Zou C, Wei N, et al. Real world emission characteristics of Chinese fleet and the current situation of underestimated ship emissions. Journal of Cleaner Production. 2023;418:138107.

[15] Tang R, Guo S, Song K, Yu Y, Tan R, Wang H, et al. Emission characteristics of intermediate volatility organic compounds from a Chinese gasoline engine under varied operating conditions: Influence of fuel, velocity, torque, rotational speed, and after-treatment device. Science of The Total Environment. 2024;906:167761.

[16] Jafarian M, Haseli P, Saxena S, Dally B. Emerging technologies for catalytic gasification of petroleum residue derived fuels for sustainable and cleaner fuel production—An overview. Energy Reports. 2023;9:3248-72.

[17] Mueller L, Jakobi G, Czech H, Stengel B, Orasche J, Arteaga-Salas JM, et al. Characteristics and temporal evolution of particulate emissions from a ship diesel engine. Applied Energy. 2015;155:204-17.

[18] Merico E, Donateo A, Gambaro A, Cesari D, Gregoris E, Barbaro E, et al. Influence of in-port ships emissions to gaseous atmospheric pollutants and to particulate matter of different sizes in a Mediterranean harbour in Italy. Atmospheric Environment. 2016;139:1-10.

[19] Park M-H, Hur J-J, Lee W-J. Prediction of oil-fired boiler emissions with ensemble methods considering variable combustion air conditions. Journal of Cleaner Production. 2022;375:134094.

[20] Yau PS, Lee SC, Corbett JJ, Wang C, Cheng Y, Ho KF. Estimation of exhaust emission from ocean-going vessels in Hong Kong. Science of The Total Environment. 2012;431:299-306.

[21] Wu B, Wang Y, Wang D, Feng Y, Jin S. Generation mechanism and emission characteristics of N2O and NOx in ammonia-diesel dual-fuel engine. Energy. 2023;284:129291.

[22] Ntziachristos L, Saukko E, Lehtoranta K, Rönkkö T, Timonen H, Simonen P, et al. Particle emissions characterization from a medium-speed marine diesel engine with two fuels at different sampling conditions. Fuel. 2016;186:456-65.

[23] Vedachalam S, Baquerizo N, Dalai AK. Review on impacts of low sulfur regulations on marine fuels and compliance options. Fuel. 2022;310:122243.

[24] Zhang Z, Zheng W, Li Y, Cao K, Xie M, Wu P. Monitoring Sulfur Content in Marine Fuel Oil Using Ultraviolet Imaging Technology. Atmosphere2021.

[25] Awoyomi A, Patchigolla K, Anthony EJ. CO2/SO2 emission reduction in CO2 shipping infrastructure. International Journal of Greenhouse Gas Control. 2019;88:57-70.

[26] Chu-Van T, Ristovski Z, Pourkhesalian AM, Rainey T, Garaniya V, Abbassi R, et al. On-board measurements of particle and gaseous emissions from a large cargo vessel at different operating conditions. Environmental Pollution. 2018;237:832-41.

[27] Sun Q, Liang B, Cai M, Zhang Y, Ou H, Ni X, et al. Cruise observation of the marine atmosphere and ship emissions in South China Sea: Aerosol composition, sources, and the aging process. Environmental Pollution. 2023;316:120539.

[28] Zhou J, Zhou S, Wang Z. Emission characteristics of particulate matter emitted from 4- and 2-stroke marine diesel engines under the background of sulfur emission reduction. Environmental Science and Pollution Research. 2023;30(12):33660-73.

[29] Shen F, Li X. Effects of fuel types and fuel sulfur content on the characteristics of particulate emissions in marine low-speed diesel engine. Environmental Science and Pollution Research. 2020;27(30):37229-36.

[30] Garaniya V, McWilliam D, Goldsworthy L, Ghiji M. Extensive chemical characterization of a heavy fuel oil. Fuel. 2018;227:67-78.

[31] Grigoriadis A, Mamarikas S, Ioannidis I, Majamäki E, Jalkanen J-P, Ntziachristos L. Development of exhaust emission factors for vessels: A review and meta-analysis of available data. Atmospheric Environment: X. 2021;12:100142.

[32] Hou W, Liu Z, Yu G, Bie S, Zhang Y, Chen Y, et al. On-board measurements of OC/EC ratio, mixing state, and light absorption of ship-emitted particles. Science of The Total Environment. 2023;904:166692.

[33] Kuye A, Kumar P. A review of the physicochemical characteristics of ultrafine particle emissions from domestic solid fuel combustion during cooking and heating. Science of The Total Environment. 2023;886:163747.

[34] Peng Y, Cai J, Feng Y, Jiang H, Chen Y. Emission characteristic of OVOCs, I/SVOCs, OC and EC from wood combustion at different moisture contents. Atmospheric Environment. 2023;298:119620.

[35] Cui M, Xu Y, Yu B, Yan C, Li J, Zheng M, et al. Characterization of carbonaceous matter emitted from residential coal and biomass combustion by experimental simulation. Atmospheric Environment. 2023;293:119447.

[36] Du J, Xu J, Zhang D, Ye S, Yuan Y. Effect of carbonaceous components of biodiesel combustion particles on optical properties. Science of The Total Environment. 2023;859:160242.

[37] Cruz-Núñez X. An approach to a black carbon emission inventory for Mexico by two methods. Science of The Total Environment. 2014;479-480:181-8.

[38] Zhang Q, Wan Z, Hemmings B, Abbasov F. Reducing black carbon emissions from Arctic shipping: Solutions and policy implications. Journal of Cleaner Production. 2019;241:118261.

[39] Sippula O, Stengel B, Sklorz M, Streibel T, Rabe R, Orasche J, et al. Particle Emissions from a Marine Engine: Chemical Composition and Aromatic Emission Profiles under Various Operating Conditions. Environmental Science & Technology. 2014;48(19):11721-9.

[40] McCaffery C, Zhu H, Karavalakis G, Durbin TD, Miller JW, Johnson KC. Sources of air pollutants from a Tier 2 ocean-going container vessel: Main engine, auxiliary engine, and auxiliary boiler. Atmospheric Environment. 2021;245:118023.

[41] Yan J, Jia B, Zhu K, Wen W, Zhang W, Bai Z, et al. Impact of combustion-derived black carbon oxidation states on optical properties and cellular metabolomics in HeLa cells: Insights into soot organics. Atmospheric Environment. 2023;314:120118.

[42] Liu X, Zheng M, Liu Y, Jin Y, Liu J, Zhang B, et al. Intercomparison of equivalent black carbon (eBC) and elemental carbon (EC) concentrations with three-year continuous measurement in Beijing, China. Environmental Research. 2022;209:112791.

[43] Jiang Y, Yang J, Gagné S, Chan TW, Thomson K, Fofie E, et al. Sources of variance in BC mass measurements from a small marine engine: Influence of the instruments, fuels and loads. Atmospheric Environment. 2018;182:128-37.

[44] Corbin JC, Gysel-Beer M. Detection of tar brown carbon with a single particle soot photometer (SP2). Atmos Chem Phys. 2019;19(24):15673-90.

[45] Zhao J, Zhang Y, Yang Z, Liu Y, Peng S, Hong N, et al. A comprehensive study of particulate and gaseous emissions characterization from an ocean-going cargo vessel under different operating conditions. Atmospheric Environment. 2020;223:117286.